October, Lisa; Corin, Kirsten; Schreithofer, Nora; Manono, Malibongwe; Wiese, Jenny

Water quality effects on bubble-particle attachment of pyrrhotite

Published in:
Minerals Engineering

DOI:
10.1016/j.mineng.2018.11.017

Published: 15/01/2019

Document Version
Publisher's PDF, also known as Version of record

Minerals Engineering 131 (2019) 230–236

Contents lists available at ScienceDirect

Minerals Engineering

journal homepage: www.elsevier.com/locate/mineng

Water quality effects on bubble-particle attachment of pyrrhotite

Lisa October[a], Kirsten Corin[a,*], Nora Schreithofer[b], Malibongwe Manono[a], Jenny Wiese[a]

[a] Centre for Minerals Research, Department of Chemical Engineering, University of Cape Town, South Africa
[b] Department of Bioproducts and Biosystems, Clean Technologies Research Group, School of Chemical Engineering, Aalto University, Finland

ARTICLE INFO

Keywords:
Froth flotation
Bubble-particle attachment
Pyrrhotite

ABSTRACT

In froth flotation, separation between the valuable and the gangue minerals comes as a result of the attachment of hydrophobic particles to air bubbles. Considering the importance of bubble formation and bubble-particle attachment, it is evident that the pulp phase facilitates the events for the most crucial requirements of successful flotation. Water forms the bulk of the pulp phase; and as a result of water scarcities in countries like South Africa, the need to recycle process water within mining operations is increasing. Hence it is of great importance to understand the effects of water quality on the vital sub-processes within the flotation process, particularly bubble-particle attachment. A novel attachment timer which allows for 396 opportunities for bubble-particle attachment was used for the bubble-particle attachments tests in this work. Three water qualities of increasing ionic strength were tested both in the presence and absence of a xanthate collector to see the effect of increasing ionic strength of synthetic plant water on the bubble-particle attachment probability. The attachment time measurements showed a general decrease in attachment probability as the ionic strength of the synthetic plant water increased both in the absence and presence of a collector. This result indicated that increasing the concentration of the ions present in synthetic plant water lowered the probability of pyrrhotite particles attaching to air bubbles. Further, adsorption studies showed that less xanthate adsorbs on the mineral surface at the highest ionic strength of synthetic plant water under study. This indicates that increases in the ionic strength of synthetic plant water hindered the xanthate adsorption on the pyrrhotite surface. Furthermore, an increase in the zeta potential of pyrrhotite with increasing ionic strength was reported, indicating cation adsorption on the mineral surface. The study presented shows a direct relationship between the zeta potential and attachment probability.

1. Introduction

With the current water scarcity in countries like South Africa, the need to recirculate process water within mining operations is becoming greater. The ionic strength of the process water however increases with each recirculation and this may affect the flotation process (Slatter et al., 2009). Considering that the most basic requirement for an effective separation is the attachment of hydrophobic particles to air bubbles, it is essential to understand how changes in water chemistry affect the bubble-particle attachment sub-process.

When a bubble and a particle approach one another and come into close contact, the liquid film between the air-water and solid-water interfaces becomes thinner. The bubble-particle attachment process begins with the thinning of the liquid film at the air-water and solid-water interfaces to critical thickness; followed by the rupturing of the liquid film as it becomes unstable, leading to the establishment of a three-phase contact line and the occurrence of bubble-particle attachment. This process is concluded when the bubble-particle contact line spreads across the surface, forming a stable wetting perimeter with equilibrium contact angles (Albijanic et al., 2010).

The attachment timers, traditionally referred to in literature as “Induction timer” instruments are commonly used to measure and predict the susceptibility of particles to float. The technique consists of a particle bed and a bubble generated at the tip of a single needle. The bubble is then brought in contact with the particle bed for a set contact time at several locations on the particle bed and this process is repeated for a range of contact times. Commonly 10 different locations are used on the particle bed and the attachment time is defined as the contact time at which the attachment probability is a certain percentage determined prior to the experiment (Albijanic et al., 2012; Glembotsky, 1953; Gu et al., 2003; Yoon and Yordan, 1991).

Within literature the terms *induction time* and *attachment time* are often used synonymously (Gu et al., 2003; Ralston et al., 1999). However, in current terminology, the attachment time is a larger concept encompassing the induction time. To avoid confusion, in this paper the authors have followed the terminology used by Albijanic et al. (2010),

* Corresponding author. Tel.: +27 21 650 2018.
E-mail address: kirsten.corin@uct.ac.za (K. Corin).

https://doi.org/10.1016/j.mineng.2018.11.017
Received 26 March 2018; Received in revised form 15 October 2018; Accepted 10 November 2018

Table 1
Concentrations of ions for the various water qualities.

Plant water type	Ca^{2+} (ppm)	Mg^{2+} (ppm)	Na^{+} (ppm)	Cl^{-} (ppm)	SO_4^{2-} (ppm)	NO_3^{-} (ppm)	CO_3^{2-} (ppm)	Total dissolved solids (mg/L)	Ionic strength (mol/L)
1 SPW	80	70	153	287	240	176	17	1023	0.0241
5 SPW	400	350	765	1435	1200	880	85	5115	0.1205
10 SPW	800	700	1530	2870	2400	1760	170	10,230	0.241

where the particle-bubble attachment occurs as a result of three sub-processes: (1) drainage and thinning of the liquid film to the critical thickness, referred to as the induction time (t_i), (2) rupture of the film and formation of a three-phase contact nucleus, referred to as rupture time (t_r), (3) expansion of the three-phase contact line from the critical nucleus radius to a stable wetting perimeter, referred to as three-phase contact time (t_{tpc}). The attachment time is expressed as follows:

$$t_{att=\_} t_i + t_r + t_{tpc} \quad (1)$$

All three of these steps need to take place for the particle to be attached to the bubble and therefore attachment will not occur if the contact time is lower than t_{att} (Albijanic et al., 2010; Evans, 1954; Verrelli et al., 2011).

The effect of water quality on induction time with a bitumen system was studied by Gu et al. (2003) and it was shown that the attachment time decreased upon the addition of Ca^{2+} to clear process water compared to without Ca^{2+}. Yoon and Yordan (1991) showed a decrease in attachment time (and hence increase in floatability) with increasing KCl concentration in a quartz-dodecylammonium hydrochloride (DAH collector) system at low DAH dosage. This was attributed to the compression of the electrical double layer in the presence of ions leading to the acceleration of the rupturing of the liquid film between the bubble and particle; ultimately decreasing the bubble-particle attachment time. An opposite trend in floatability was observed by these authors with an increase in collector dosage under constant water conditions; this was said to be resulting from the collector ions associating with one another and their subsequent adsorption on the mineral surface in bimolecular layers. Thus, from previous studies conducted in this area, it is clear that there is little knowledge regarding the effect of plant water of increasing ionic strength on the bubble-particle attachment process in sulfide minerals.

Platinum bearing ores from the Merensky reef consist of approximately 1% sulfides and about 45% of the sulfide is pyrrhotite (Liddell et al., 1986); making pyrrhotite the main sulfide mineral in the Merensky reef. Pyrrhotite however readily oxidizes to ferric hydroxide under conventional flotation conditions, pH 9 and open to the atmosphere (Miller, 2005). Both the natural and induced hydrophobicity of pyrrhotite have been widely studied and factors such as oxidation potential, pH and activation have been shown to have significant effects on pyrrhotite flotation (Hodgson and Agar, 1984; Miller, 2005; Montalti, 1994; Peters, 1977). The effect of ionic strength on pyrrhotite flotation is however unclear.

Thus, the aim of this study was to assess the bubble-particle attachment probability of pyrrhotite under synthetic plant water of increasing ionic strength both in the presence and absence of a collector. It should be noted that the ions could also affect the bubble surface. A study by Takahashi (2005) showed that with increasing concentration of NaCl the zeta potential of the bubble decreased while the zeta potential decreased even more so with increasing concentration of $MgCl_2$. This work is however focussed on the effect of ions in solution on the particle surface.

The experiments were done by the means of the Automated Contact Time Apparatus described by Jávor et al. (2016); Aspiala et al. (2018) elsewhere and a brief description of its operation will be given in the next section.

2. Materials and experimental procedures

2.1. Materials

The pyrrhotite used in this investigation was obtained from Ward's Science. 1 kg of pyrrhotite sample was hammered manually to 100% passing 1000 μm. The crushed sample was then pulverized and subsequently sieved through 75 and 38 μm sieves. The fraction of particles greater than 75 μm was then re-pulverized such that the size fraction of the entire sample was < 75 μm. This sample was purged with nitrogen and refrigerated. Upon arrival at Aalto University the pyrrhotite particles of −75 + 38 μm were split into 10 samples using a rotary splitter. The samples were purged with argon and stored in bottles in a refrigerator.

Both purified water and synthetic plant waters were used for the attachment timer measurements. Synthetic plant water (1 SPW) as described by Wiese et al. (2005) was used as the water quality with low ionic strength and to simulate a recirculation of this synthetic plant water, the content of dissolved solids was increased 5 and 10 times, and are referred to as 5 SPW and 10 SPW respectively. Table 1 gives an account of the concentrations of the various ions in the synthetic plant waters tested. This is without any collector in the system, noting that both the TDS and ionic strength would be practically the same in both cases with and without collector. The properties of the purified water used are shown in Table 2.

The salts used for preparation of the synthetic plant waters were of analytical grade, while the SIBX was 97% purity.

2.2. Attachment time measurements

2.2.1. Experimental setup

The Automated Contact Time Apparatus used in this investigation was described by Jávor et al. (2016) and Aspiala et al. (2018) elsewhere, therefore only a brief description of its operation will be given below. The main advantage of the instrument is, that it allows the collection of a large amount of data for statistical analysis within a relatively short time period. Previously authors have chosen to measure 10 particle-bubble contacts per condition with commonly used attachment timers (Albijanic et al., 2011; Gu et al., 2003; Yoon and Yordan, 1991), while the Automated Contact Time Apparatus allows for 396 contacts within the particle bed hence providing 396 opportunities for bubble-particle attachment. Furthermore, the particles that successfully attach to the bubbles are collected in a collection bin and can be analysed further in terms of shape, composition, size and mass recovered.

The Automated Contact Time Apparatus housed at Aalto University shown on Fig. 1.

Table 2
Properties of purified water.

Ultra-pure water	Resistivity at 25 °C (MΩ·cm)	Conductivity (μs/cm)	Total organic carbon (ppb)	Na^{+}(ppb)	Cl^{-} (ppb)
	18.2	< 0.055	< 5	< 1	< 1

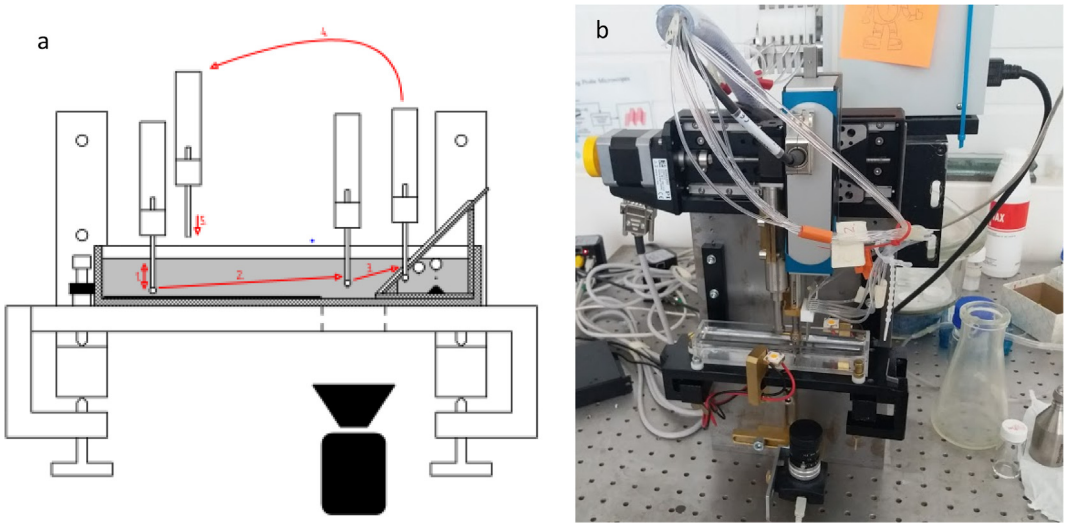

Fig. 1. (a) Schematic of the attachment timer (Aspiala et al., 2018), (b) photograph of the Automated Contact Time Apparatus.

The instrument consists of six needles with each needle generating a bubble with set diameter; once the bubbles are generated they are brought into contact with the particle bed for a set contact time. The needles are then automatically lifted and moved to the area where an image of the bubble-particle aggregates is taken; LED lights located at both sides of the pool light up as the picture is taken in order to obtain clear images suitable for analysis. After the image is taken the needles with the bubble-particle aggregates are automatically transferred to the particle collection bin, where additional air is pumped through the needles to release the bubble-particle aggregates. After this deposition the needles then automatically move to the next 1 mm of the particle bed. This process is repeated such that the complete length of the particle bed is given an opportunity for bubble-particle attachment; resulting in a total of 66 cycles with 396 bubble-particle contacts per experiment.

Prior to the start of the 66 measurement cycles certain parameters are set on the experimental controller programme. These parameters included the contact time, approach distance, approach velocity, detachment velocity, retreat distance, bubble size, compression and pumping time. Although the volume of air used to generate the bubbles is set on the experimental controller programme, the reported bubble size in this device is largely dependent on the chemical environment within the cell such as the ionic strength of the water investigated. Consequently, parameters such as the compression with the particle bed, approach and retreat distance which are dependent on bubble size may also differ slightly from what was set. However, the actual measured values of these parameters for each cycle are given upon the completion of the 66 cycles.

The digital camera situated below the cell takes two images of the bubble-particle aggregate at the tip of the needle for each cycle. The first image with white light illumination is used to determine the bubble size, Fig. 3. An optical fibre is located inside each of the six needles attached to a green LED which lights the bubbles from the inside, Fig. 2. This creates a good contrast that facilitates the automatic detection of attached particles to the bubbles. All the images of the 66 cycles are saved.

All measurements were done in duplicate in a random order to minimise experimental error.

2.2.2. Sample and particle bed preparation

A slurry was made with 9 g pyrrhotite and 100 ml of the particular water type under investigation. Experiments were performed both in the presence and absence of a collector. When a collector was utilised, the slurry was conditioned for 2 min with 100 g/t (standard industry dosage) sodium isobutyl xanthate collector (SIBX), thereafter it was allowed to settle for approximately 3 min. The liquid at the top was removed with a pipette and filtered with a glass funnel and filter paper such that a clear water was obtained and only a thin layer of liquid above the settled particles was left in the flask. The clear liquid was transferred to the cell of the attachment timer and the settled particles were used to make the particle bed.

Once the liquid pool was ¾ full, a heap of particles was introduced. An automated shovel attached to the linear actuator was then used to obtain a flat particle bed of a pre-set bed height. More particles were added to fill the length of the pool; and between each addition of particles the shovel controller was employed until a flat particle bed of 2 mm was obtained. The bed height is arbitrary, but the approach distance and bubble size were chosen based on the bed height, such that sufficient compression of the bubbles with the particle bed was achieved. The particle collection bin was then inserted into the cell.

2.2.3. Adsorption studies

A slurry of 9 g pyrrhotite and 100 ml of the particular synthetic plant water was made. 90 µL of 1% SIBX solution was added to the slurry which is equivalent to the addition 100 g of xanthate per tonne of pyrrhotite; resulting in a slurry with 10 ppm xanthate. The slurry was then placed in a temperature-controlled water bath (25 °C) for 20 min; stirred at 450 rpm. A 0.45 µm filter was attached to a syringe to draw 3 ml of solution. The absorbance of the clear solution was measured with UV–VIS spectrophotometer at 301 nm. A calibration curve was constructed using the absorbance of xanthate at known concentrations; therefore, the concentration of xanthate in the clear solution could be calculated. All measurements were done in triplicate to minimise experimental error.

2.3. Zeta potential measurements

Very dilute mixtures of the particular water type and pyrrhotite particles were made up; the dilute mixtures were then equally divided in six containers and the pH was adjusted to 2, 4, 6, 8, 10 and 12 with dilute HCl or dilute NaOH. After 15 min on the magnetic stirrer the pH was measured again and adjusted where needed. 1 ml of the suspension was then transferred to the Malvern Dip Cell and inserted in the Malvern ZetaSizer where measurements were taken. All zeta potential measurements were performed in triplicate to reduce experimental error.

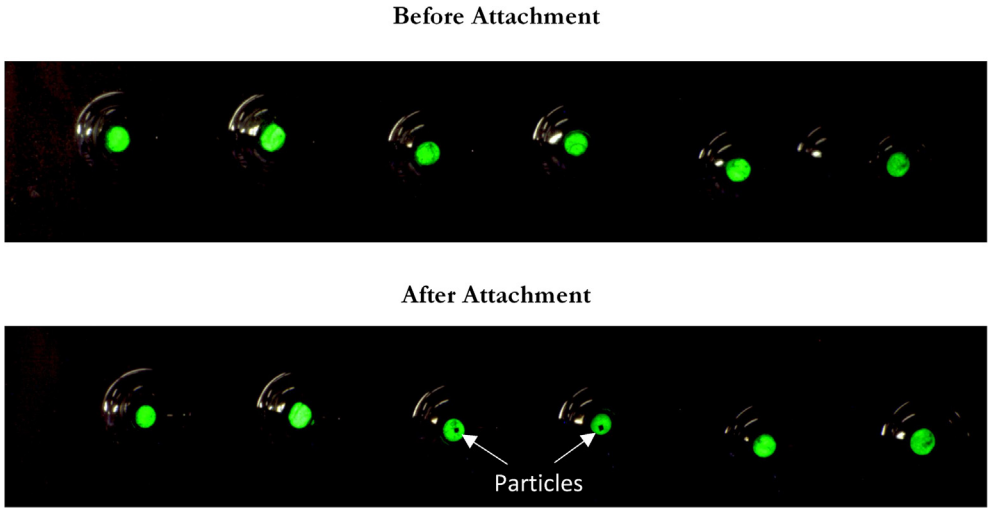

Fig. 2. Image of the array generated for bubble-particle attachment detection.

3. Results and discussion

The images generated were studied to establish the bubble-particle attachment probability for the different water qualities tested. Fig. 2 shows an example of an image before attachment and after a measurement cycle.

Fig. 2 shows that there was attachment of particles occurring at two of the six bubbles (indicated by the black dots at the surface of the bubbles generated by needles three and four, from left to right). Therefore, for this cycle the probability of attachment was 2/6 (i.e. 33.33%) The 66 images obtained per condition investigated were studied in this way to quantify the probability of bubble-particle attachment under water of increasing ionic strength.

Fig. 3 shows the first image taken, which is used to determine the bubble size. The bubble size is determined by applying a pre-calibrated circle finding programme; details in Aspiala et al. (2018) Fig. 4 shows the identification lines added by the programme used to determine the bubble size.

3.1. The effect of water quality on attachment probability in the presence of a collector

The actual bubble sizes generated by each needle for the 66 cycles was returned by the experimental programme. Fig. 5 depicts the bubble size distribution averaged across the two contact times (100 ms and 200 ms) for every water quality tested. This could be done as the contact time chosen is not expected to change the size of the bubble generated by the Automated Contact Time Apparatus used in this work.

The bubble size distribution in Fig. 5 shows that the largest modal bubble size was generated with purified water (1.75 mm), while the smallest modal bubble size was generated with 10 SPW (1.65 mm).

The overall attachment probability is presented in Fig. 6 and is essentially the percentage attachment achieved over the 396 bubble-particle contacts.

Fig. 6 shows the attachment probability using purified water and the three synthetic plant waters of increasing ionic strength at contact times 100 ms and 200 ms. The attachment probability was greater at a contact time of 200 ms across all the water qualities investigated, this result was expected as the longer the bubble is in contact with the particle bed the greater the opportunity for particles to attach to the bubbles. The results shown in Fig. 6 show that the overall average attachment probability decreases with deteriorating water quality. The attachment probability of purified water at 200 ms was not tested, it was clear that the highest attachment probability is achieved with a higher contact time as the bubble is in contact with the particle bed for longer. The ultra-purified water was thus merely used as a baseline to see the effect with no ions in solution.

It was expected that with an increase in ionic strength of plant water the floatability of the mineral would increase as explained by the electrical double layer theory (Laskowski and Iskra, 1970; Yoon and Yordan, 1991). Hodgson and Agar (1989) indicated that Ca^{2+} increased the amount of xanthate necessary to create a hydrophobic pyrrhotite surface; suggesting that the presence of Ca^{2+} induces hydrophilicity. Moreover, Ikumapayi et al. (2012) described the decrease in galena recovery with increasing Ca^{2+} to be as a result of Ca^{2+} inhibiting the adsorption of xanthate on the mineral surface. Additionally, Kirjavainen et al. (2002) found that calcium and thiosulfate ions had a negative effect on the floatability of sulfides in the absence of iron ions that are leached into solution during milling. It was thus speculated that the reduction in attachment probability as the ionic strength of water was increased as observed in Fig. 6 was as a result of the increasing concentration of ions such as Ca^{2+}, which inhibited the adsorption of xanthate on the mineral surface. This could further be supported by the fact that the attachment probability was highest in purified water.

3.2. Adsorption of xanthate

Fig. 7 shows the concentration of xanthate left in solution and adsorbed on the mineral surface at the different synthetic plant water qualities. An increase in xanthate concentration in solution is observed with an increase in ionic strength of the synthetic plant water. This indicates that less xanthate adsorbs on the mineral surface as the ionic strength increases. However, considering that xanthate concentration in the pyrrhotite slurry was 10 ppm, the amount of xanthate that adsorbed

Fig. 3. Image used to determine bubble size.

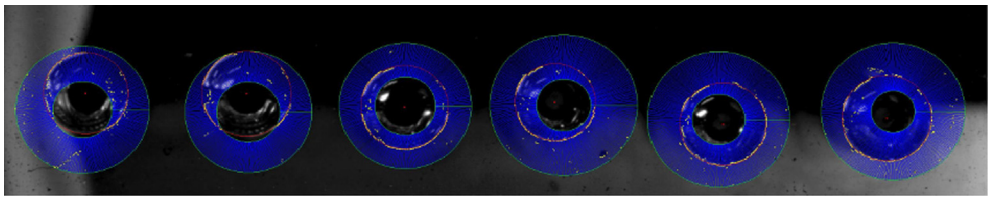

Fig. 4. Identification lines added by programme to determine bubble size.

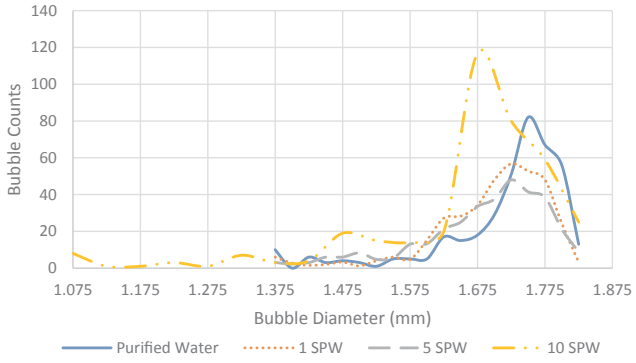

Fig. 5. Bubble size distribution for the various water qualities with SIBX collector.

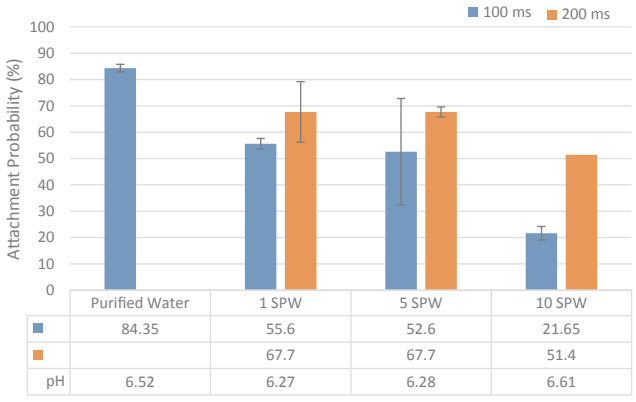

Fig. 6. Overall attachment probability of different water qualities with collector (SIBX).

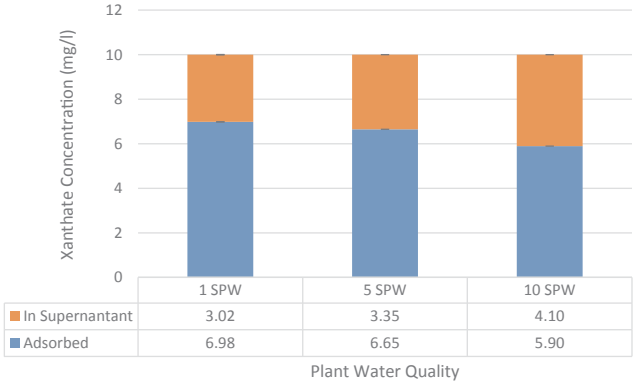

Fig. 7. Concentration of xanthate adsorbed on mineral and left in solution at various synthetic plant water qualities.

is not significantly different across the three synthetic plant waters. Previous studies have shown that the addition of ionic collector to an electrolyte solution results in a further increase in the ionic strength which will lower the concentration of collector required to form hydrophilic micelles at the mineral surface (Laskowski, 2013; Evans and Wennerström, 1994). Studies have also shown that insoluble complexes form between the collector and ions, reducing the amount of xanthate available for adsorption on the mineral surface (Fuerstenau and Somasundaran, 2003). 10.8% more xanthate is adsorbed with 1 SPW compared to with 10 SPW which does indicate the deterring of xanthate adsorption on pyrrhotite at synthetic plant water of high ionic strength.

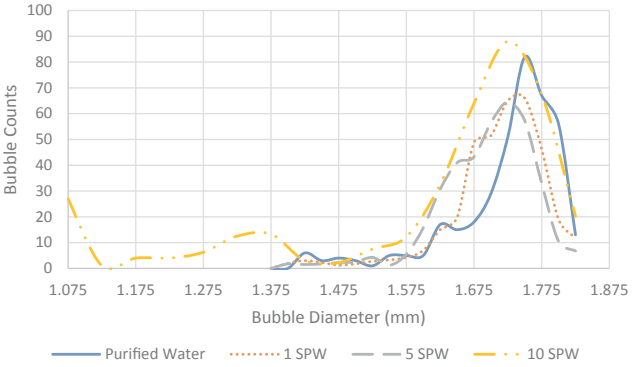

Fig. 8. Bubble size distribution for the various water qualities with no collector.

3.3. The effect of water quality on attachment probability in the absence of a collector

Fig. 8 gives an account of the bubble size distribution averaged across the two contact times (100 ms and 200 ms) for every water quality tested with no collector in the system.

Similarly, as in Fig. 5 the modal bubble size tends to decrease as the ionic strength of plant water increased. Furthermore, multimodal profiles were observed for 10 SPW either indicating an insufficient number of measurements taken or that different competing mechanisms were simultaneously at play.

Fig. 9 summarises the attachment probability at the modal bubble size for each of the water qualities investigated.

The natural pH of this system was measured to be between 6.27 and 6.61 and it is evident that attachment does indeed occur in this pH

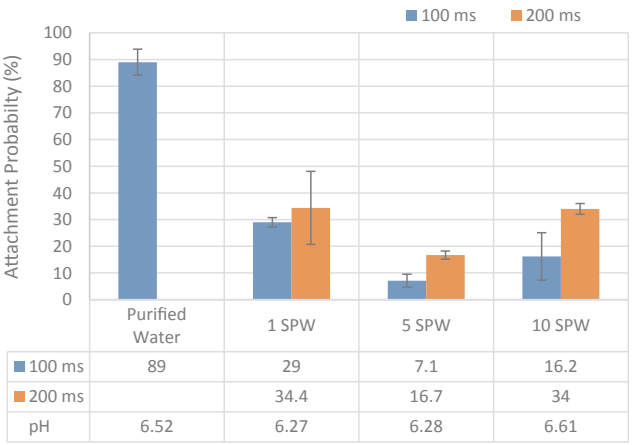

Fig. 9. Attachment probability at the modal bubble size in the absence of a collector.

range. This result was contrary to the findings of Miller (2005) where contact angle measurements showed that the hydrophilic state of pyrrhotite stabilized (contact angle of zero) at pH values above 4.5 in the absence of collector. However, it has been reported that elemental sulfur is a product of pyrrhotite oxidation (Steger and Desjardins, 1978; Steger, 1982; Belzile et al., 2004) which is hydrophobic and can remain stable for long periods (Miller, 2005). The sulfur at the pyrrhotite surface could thus be the reason for the observed floatability of pyrrhotite in this pH range.

According to the electrical double layer theory as previously stated, an increase in ionic strength of the solution should increase the floatability of the mineral but Fig. 9 shows a general decrease in the probability of attachment of pyrrhotite particles to air bubbles with an increase in the concentration of dissolved solids. The surface of pyrrhotite is known to oxidize rapidly when exposed to air and results in the surface of the mineral being covered with ferric hydroxide (Miller, 2005); rendering the mineral hydrophilic. This phenomenon will undoubtedly hinder any activation reaction from occurring on the surface of the mineral and could possibly obstruct the expected effect of the electrical double layer.

The flotation of pyrrhotite is recognised to be very complicated and is influenced mainly by oxidation potential and pH. The plant water with an intermediate level of ionic strength tends to show a lower probability for the attachment of pyrrhotite particles to the bubbles. This result could potentially be explained by a combined effect of pH, oxidation potential and electrolytes in the system yielding a minima in attachment probability.

Upon comparison between Figs. 6 and 9 it is clear that the attachment probability is higher in the presence of a collector as opposed to without a collector for all the synthetic plant water tested. This result was expected as the primary role of a collector is to induce hydrophobicity on the valuable mineral particles. The result of SIBX collector enhancing the hydrophobicity of pyrrhotite was thus strengthened even in this static bubble-particle attachment system.

3.4. Zeta potential measurements

Fig. 10 gives an account of the zeta potential of pyrrhotite in the 4 water qualities tested over a pH range of 2 to 12. It is evident that the pyrrhotite particles in purified water resulted in the most negative zeta potential, while generally the zeta potential of pyrrhotite tends to increase with increasing ionic strength; indicating possible adsorption of the specific metal cations on the mineral surface (Moignard *et al.*, 1977). The effect of the indifferent ions is evident in Fig. 10 in terms of modifying the magnitude of the zeta potential by compression of the electrical double layer. The compression of the electrical double is evident as the magnitude of the zeta potential of pyrrhotite decreases (becomes more positive) with increasing ionic strength. The results obtained in Fig. 9 also demonstrates that at higher ionic concentrations, the ions cover the mineral surface to a greater extent and hence increase its potential. It is expected that as the zeta potential of the mineral surface is increased the repulsion between the particles and air bubbles will be reduced; which should result in an increased bubble-particle attachment.

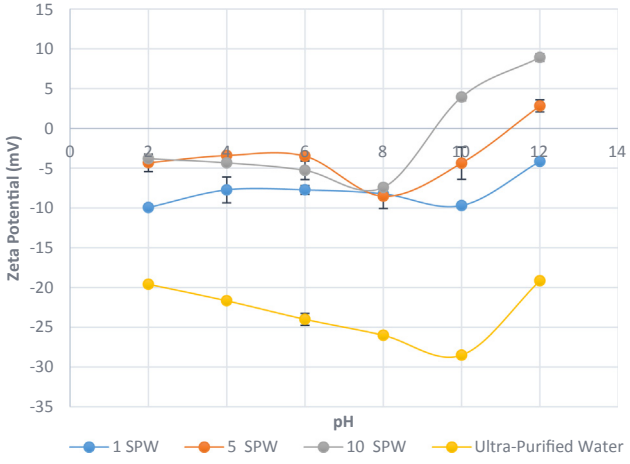

Fig. 10. Zeta Potential of Pyrrhotite in the Various Water Qualities.

The results obtained from this study however shows that pyrrhotite particles with a more negative zeta potential result in a higher attachment probability. This could be due to the zeta potential of the bubble also changing in the presence of the various ionic solutions. A study by Yang et al. (2001) showed that the zeta potential is dependent not only on the solution pH, but also on the concentration of electrolytes and type of metal ions present in the system. NaCl was found to decrease the zeta potential towards more negative values, while multivalent metal ions Ca^{2+} and Al^{3+} had a greater impact on the magnitude of the zeta potential and can even reverse the charge polarity. Similar findings were reported by Takahashi (2005) with regard to NaCl, showing that the zeta potential increased even more so with increasing concentration of $MgCl_2$. Furthermore, the passivation of the mineral surface by the ions could possibly have a depressing effect, resulting in the low attachment probability achieved by the pyrrhotite particles in solutions of high ionic strength. Zeta potential values close to 0 mV tend to indicate strong agglomeration and precipitation in the suspension (Salopek et al., 1992) and hence could explain the lower attachment observed with plant water of high ionic strength.

As previously stated the tests were carried out at pH values of 6.27–6.61 (the natural pH of the system); the zeta potential measurements at this pH range show that the zeta potential of the pyrrhotite in 5 SPW is slightly higher than it is at 10 SPW. This result could possibly explain the low attachment probability achieved with 5 SPW as seen in Fig. 7.

4. Conclusions

The results presented in this study generally show a decrease in the attachment probability of pyrrhotite to air bubbles as the ionic strength of synthetic plant water is increased both in the presence and absence of a collector. Further, the attachment probability across all water qualities was higher in the presence of SIBX compared to without the collector. Previous studies have shown that Ca^{2+} increases the amount of xanthate required to create a hydrophobic pyrrhotite surface and adsorption studies in this work indicated that more xanthate is left in solution at the highest ionic strength tested. This indicates that less xanthate adsorbs on the pyrrhotite surface with synthetic plant water of higher ionic strength.

Furthermore, it is well known that pyrrhotite readily oxidises when exposed to the atmosphere, resulting in ferric hydroxide formation on the mineral surface. In the absence of a collector this trend may possibly be due to the joint effects of oxidation, pH and ionic strength; individually these factors are known to affect the natural flotation of pyrrhotite. Zeta potential measurements have shown a general increase in zeta potential of pyrrhotite as the ionic strength of the water is increased. This indicates an increase in the adsorption of cations on the mineral surface at high ionic strengths; and this may cause the lower attachment probability as the ionic strength of plant water increases.

Acknowledgements

Funding for this research was provided by the National Research Foundation of South Africa (South Africa) (NRF) [Grant number 103641] and Academy of Finland Mineral Resources and Material Substitution MISU program (Finland) – Protocol development for evaluation of water-saving alternatives in minerals processing – “Bridging North to South” project. Any opinion, finding and conclusion or

recommendation expressed in this material is that of the authors and the NRF does not accept any liability in this regard. Further the financial and technical contributions from the South African Minerals to Metals Research Institute (SAMMRI) is also acknowledged.

References

Albijanic, B., Amini, E., Wightman, E., Ozdemir, O., Nguyen, A.V., Bradshaw, D., 2011. A relationship between the bubble–particle attachment time and the mineralogy of a copper–sulphide ore. Miner. Eng. 24, 1335–1339.

Albijanic, B., Bradshaw, D.J., Nguyen, A.V., 2012. The relationships between the bubble–particle attachment time, collector dosage and the mineralogy of a copper sulfide ore. Miner. Eng. 36, 309–313. https://doi.org/10.1016/j.mineng.2012.06.007.

Albijanic, B., Ozdemir, O., Nguyen, A.V., Bradshaw, D., 2010. A review of induction and attachment times of wetting thin films between air bubbles and particles and its relevance in the separation of particles by flotation. Adv. Colloid Interface Sci. 159, 1–21. https://doi.org/10.1016/j.cis.2010.04.003.

Aspiala, M., Schreithofer, N., Serna-Guerrero, R., 2018. Automated contact time apparatus and measurement procedure for bubble-particle interaction analysis. Miner. Eng. 121, 77–82. https://doi.org/10.1016/j.mineng.2018.02.018.

Belzile, N., Chen, Y., Cai, M., Li, Y., 2004. A review on pyrrhotite oxidation. J. Geochem. Explor. 84, 65–76.

Evans, L.F., 1954. Bubble-mineral attachment in flotation. Ind. Eng. Chem. 46, 2420–2424.

Evans, D.F., Wennerström, H., 1994. Structure and Properties of Micelles, The Colloidal Domain - where Physics, Chemistry, Biology, and Technology Meet. VCH Publishers, New York.

Fuerstenau, M.C., Somasundaran, P., 2003. Flotation. In: Fuerstenau, M.C., Han, K. (Eds.), Principles of Mineral Processing. Society for Mining, Metallurgy, and Exploration (SME), Littleton, Colorado, pp. 245–306.

Glembotsky, V.A., 1953. The time of attachment of bubbles to solid particles in flotation and its measurement. Lzv. Akad. Nauk SSSR 11, 1524–1531.

Gu, G., Xu, Z., Nandakumar, K., Masliyah, J., 2003. Effects of physical environment on induction time of air–bitumen attachment. Int. J. Miner. Process. 69, 235–250. https://doi.org/10.1016/S0301-7516(02)00128-X.

Hodgson, M., Agar, G.E., 1984. An electrochemical investigation into the natural flotability of pyrrhotite. In: Richardson, P.R., Srinivasan, S.S., Woods, R. (Eds.), Electrochemistry in Mineral and Metal Processing. ECS, Pennington, NJ, USA, pp. 185–201.

Hodgson, M., Agar, G.E., 1989. Eilectrochemical investigations into the flotation chemistry of pentlandite and pyrrhotite: process water and xanthate interactions. Can. Metall. Q. 28, 189–198. https://doi.org/10.1179/cmq.1989.28.3.189.

Ikumapayi, F., Makitalo, M., Johansson, B., Rao, K.H., 2012. Recycling of process water in sulphide flotation: effect of calcium and sulphate ions on flotation of galena. Miner. Eng. 39, 77–88. https://doi.org/10.1016/j.mineng.2012.07.016.

Jávor, Z., Schreithofer, N., Heiskanen, K., Serna, R., 2016. Technical Note on the Development of a New Attachment Timer for Predicting the Change in Ore Floatability. In: Proceedings of the XXVIII International Mineral Processing Congress (IMPC 2016), September 11-15, 2016. Canadian Institute of Mining, Metallurgy and Petroleum, Québec City.

Kirjavainen, V., Schreithofer, N., Heiskanen, K., 2002. Effect of some process variables on flotability of sulfide nickel ores 65, 59–72.

Miller, J.D., 2005. A review of pyrrhotite flotation chemistry in the processing of PGM ores. Miner. Eng. 18 (18), 855–865. https://doi.org/10.1016/j.mineng.2005.02.011.

Montalti, M., 1994. Interaction of Ethyl Xanthate with Pyrite and Pyrrhotite Minerals. University of South Australia.

Laskowski, J., Iskra, J., 1970. Role of capillary effects in bubble-particle collision in flotation. Trans. Inst. Min. Metall. 79, C6.

Laskowski, J.S., 2013. From amine molecules adsorption to amine precipitate transport by bubbles: a potash ore flotation mechanism. Miner. Eng. 45, 170–179.

Liddell, K. S., McRae, L. B., Dunne, R.C., 1986. Process routes for beneficiation of noble metals from Merensky and UG-2 ores. Mintek Review No. 4, Randburg.

Peters, E., 1977. In: Rand, D.A.J., Welsh, B.J. (Eds.), Trends in Electrochemistry. Plenum Press, NY, 267.

Ralston, J., Fornasiero, D., Hayes, R., 1999. Bubble–particle attachment and detachment in flotation. Int. J. Miner. Process. 56, 133–164. https://doi.org/10.1016/S0301-7516(98)00046-5.

Salopek, B., Krasic, D., Filipovic, S., 1992. Measurement and Application of Zeta-Potential. Rudarsko-Geolosko-Naftni Zbornik 4, 147–151.

Slatter, K.A., Plint, N.D., Cole, M., Dilsook, V., De Vaux, D., Palm, N., Oostendorp, B., 2009. Water Management in Anglo Platinum Process Operations: Effects of Water Quality on Process Operations. In: Abstracts of the International Mine Water Conference, Pretoria, South Africa, 19th – 23rd October 2009 Proceedings ISBN Number: 978-0-9802623-5-3. pp. 46–55.

Steger, H.F., Desjardins, L.E., 1978. Oxidation of sulphide minerals: 4. Pyrite, chalcopyrite and pyrrhotite. Chem. Geol. 23, 225–237.

Steger, H.F., 1982. Oxidation of sulfide minerals: VII. Effect of temperature and relative humidity on the oxidation of pyrrhotite. Chem. Geol. 35, 281–295.

Takahashi, M., 2005. ζ Potential of microbubbles in aqueous solutions: electrical properties of the gas − water interface. J. Phys. Chem. B 109, 21858–21864. https://doi.org/10.1021/jp0445270.

Verrelli, D.I., Koh, P.T.L., Nguyen, A.V., 2011. Particle–bubble interaction and attachment in flotation. Chem. Eng. Sci. 66, 5910–5921. https://doi.org/10.1016/j.ces.2011.08.016.

Wiese, J., Harris, P., Bradshaw, D., 2005. The influence of the reagent suite on the flotation of ores from the Merensky reef. Miner. Eng. 18, 189–198. https://doi.org/10.1016/j.mineng.2004.09.013.

Yang, C., Dabros, T., Li, D., Czarnecki, J., Masliyah, J.H., 2001. Measurement of the zeta potential of gas bubbles in aqueous solutions by microelectrophoresis method. J. Colloid Interface Sci. 243, 128–135. https://doi.org/10.1006/jcis.2001.7842.

Yoon, R.-H., Yordan, J.L., 1991. Induction time measurements for the quartz-amine flotation system. J. Colloid Interface Sci. 141, 374–383. https://doi.org/10.1016/0021-9797(91)90333-4.